

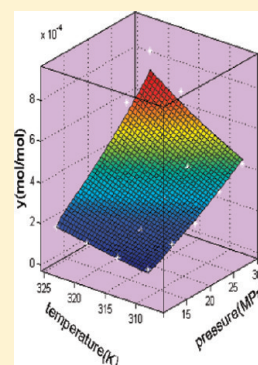
Solubility and Micronization of DL-2-Phenoxypropionic Acid in Supercritical CO₂

Kaili Zhou,[†] Yongbing Liu,[†] Chunyue Pan,[‡] and Jianmin Yi^{*,†}

[†]Department of Chemical Engineering, Hunan Institute of Science and Technology, Yueyang 414000, Hunan, China

[‡]College of Chemistry and Chemical Engineering, Central South University, Changsha 410083, Hunan, China

ABSTRACT: To understand the process of DL-2-phenoxypropionic acid fine particles formation with rapid expansion of supercritical solution (RESS), it is vital to determine the solubility of DL-2-phenoxypropionic acid at different operation conditions and to detect an empirical model to correlate the solubility data. In this investigation, solubility in supercritical carbon dioxide (SC-CO₂) was measured by a static method with the pressure ranged from (10 to 30) MPa and temperature from (308 to 323) K. Chrastil and its modified models have better correlation effects than the Mendez-Santiago and Teja model, especially the Adachi and Lu modified Chrastil model, provides a nearly perfect average absolute relative deviation (AARD) of 0.0532. Then, RESS was applied to prepare DL-2-phenoxypropionic acid microstructures. The effects of the extraction temperature ((308 to 328) K), extraction pressure ((10 to 30) MPa), spray distance ((10 to 30) mm), nozzle temperature ((343 to 383) K), and nozzle diameter ((0.1 to 0.4) mm) were searched on morphology and size of the microstructures. On the basis of the different experimental conditions, filaments with the diameter of (1 to 15) nm were obtained, which entwine into a mesh pattern and even are accompanied with flakes or particles in some cases. The micronization result indicates a general trend that the higher supersaturation at some operation conditions, the smaller the filaments observed.



■ INTRODUCTION

Supercritical fluids processes provide practicable and attractive approaches for fine particles manufacture, such as antisolvent processes (gas antisolvent (GAS)), rapid expansion of supercritical solution (RESS), and particles from gas-saturated solutions/suspensions (PGSS). They can present micro- even nanoparticles with narrow size distribution.¹ RESS, an appealing alternative for the formation of fine particles in the aforementioned applications, has been explored recently with great interest because solvent-free microparticles with controllable particle size can be produced.^{2–4} The shape, surface topography, and size distribution of RESS productions are bound up with the chemical structure of material and extraction conditions, expansion parameters, spray distance, and nozzle design.^{5–9} Solubility of solid solute in supercritical CO₂ is

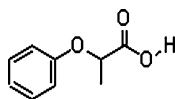


Figure 1. Chemical structure of DL-2-phenoxypropionic acid.

essential information for the RESS process since the degree of supersaturation determines the rates of nucleation and growth, and consequently influences strongly on the particle size and morphology. In addition, an insufficient solubility limits the practical applicability.⁹ DL-2-phenoxypropionic acid (Figure 1) was used as an interesting substance in this study. DL-2-phenoxypropionic acid is a light yellow crystalline powder and insoluble in water. It contains both a phenoxy and a carboxyl

group, which can easily react with an alcohol. It is used most widely as an intermediate for pharmaceuticals. Specific surface area and particle size are important properties to a solid substance for its restrictions on the practical applicability. On all accounts, it seemed rewarding to study the solubility and RESS of DL-2-phenoxypropionic acid.

The main objective of this project was to obtain the relationship between the solubility of DL-2-phenoxypropionic acid and the morphology and size of the particles precipitated by RESS. Therefore, the first series of experiments in this investigation was performed to study the effect of pressure and temperature on the solubility of DL-2-phenoxypropionic acid in SC-CO₂. Then, the experimental data of solubility were correlated with the Chrastil model, modified Chrastil models, and Mendez-Santiago and Teja model. In the second series of the experiments, RESS was applied to prepare DL-2-phenoxypropionic acid microstructures.

■ EXPERIMENTAL SECTION

Materials. DL-2-phenoxypropionic acid (CAS Registry No. 940–31–8, 0.98 mol purity, GC grade, made in New Jersey, USA) was used as the solute. Absolute ethanol (CAS Registry No. 64–17–5, 0.997 mol purity, GC grade), supplied by Tianli Chemical Reagent CO., Ltd., was used as a solvent to collect the extract. High purity CO₂ (CAS Registry No. 124–38–9,

Received: October 12, 2011

Accepted: January 9, 2012

Published: February 3, 2012

greater than 0.999 vol purity, SFC grade) was supplied by Yueyang MingZhuo Gas Co Ltd.

Equipment Apparatus. In this study, the solubility of DL-2-phenoxypropionic acid in SC-CO₂ was measured employing a static method, and DL-2-phenoxypropionic acid microstructures were manufactured using RESS. The schematic diagram of the apparatus is shown in Figure 2. It is composed mainly of

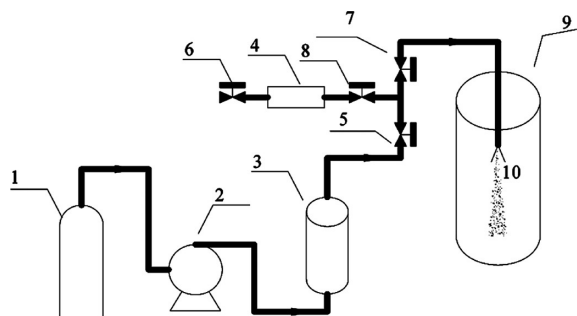


Figure 2. Schematic diagram of the experimental apparatus: 1, CO₂ cylinder; 2, plunger pump; 3, extraction cell; 4, collection vessel; 5,6,7,8, valve; 9, expansion chamber; 10, nozzle.

a carbon dioxide cylinder, a plunger pump, an extraction cell with a circulating water system and a pressure gauge, a collection vessel for solubility determination, and an expansion chamber equipped with nozzles of different diameters for RESS. The total vessel and coil between extraction column and collecting vessel (nozzle) were encircled with heating tape. The temperature of the circulating water system was controlled by a temperature controller (Jiangshu Jinzhao Temperature Instrument Company) and was monitored by a Pt resistance with an uncertainty of better than 0.1 K. The pressure gauge was composed of a pressure transducer and an indicator (Changzhou, Jiangshu, Tianli Control Instrument Manufacture Co Ltd.). Its uncertainty was 0.5 MPa in the pressure range of (0 to 50) MPa. The maximum working pressure and temperature of the system are 50.0 MPa and 373.0 K, respectively. The nozzle was equipped with a separate oil bath with a thermocouple (Jiangshu Jinzhao Temperature Instrument Company) for controlling the temperature of the nozzle inlet. The first thing of all the experiments is to determine the solubility of naphthalene in SC-CO₂ with this apparatus at the beginning, so as to make sure it was viable to get the experimental results using this apparatus. Then, the liquid CO₂ in the cylinder was pumped into the extraction cell (5 L), where excess DL-2-phenoxypropionic acid was placed previously. It was maintained at the desirable temperature and pressure for at least 3 h. When the solubility was measured, valve 7 was closed and the mixed critical fluids entered the collection vessel, the volume of which was known as 41.5 mL. At the same time, the CO₂ was slowly pumped into the extraction cell at rate of 1 L·min⁻¹, so as to keep the pressure at the fixed point. Then, the solutes within the collection vessel were dissolved with a certain amount of ethanol. The DL-2-phenoxypropionic acid concentration of the aforementioned

solution could be measured by using an ultraviolet spectrophotometer. The accuracy of absorbance was ± 0.1 %. In order to get the believable values, every measurement was repeated three times. While when the particle was prepared by RESS, valve 7 was opened and 8 was closed, making the fluids pass through the nozzle into the ambient environment in the expansion chamber. Electron micrographs of fine particles were obtained using a scanning electron microscope (JSM-6360, UK) operating at 25 kV.

RESULTS AND DISCUSSION

Solubility Determination. There is a comparison of the experimental solubility about naphthalene in SC-CO₂ with values in the existing literature¹⁰ in Table 1. The consistency among them means the complete set of apparatuses is reliable.

The experimental equilibrium solubility data of DL-2-phenoxypropionic acid in pure SC-CO₂ together with the density of carbon dioxide at all the operation conditions are shown in Table 2. Each experimental data is an average value of three experimental solubility measurements. The density data of carbon dioxide were calculated by the PR equation using Matlab as the following expression:¹¹

$$P = \frac{RT}{V - b} - \frac{a(T)}{V(V + b) + b(V - b)} \quad (1)$$

As shown in Figures 3 and 4, the solubility increases with the increase of pressure at each constant temperature and rises with the increase of temperature at a fixed pressure, rather than exhibiting a crossover phenomena as demonstrated by Jinlong Fan.¹²

In order to understand the relationship between solubility and temperature (or pressure) better, it is necessary to introduce a solubility correlate equation. Because the values of physical properties and/or critical data of most solid solutes are unavailable for the thermodynamic model, the empirical models are used more widely. The Chrastil model and Mendez-Santiago and Teja model are two common empirical models, which correlate the solubility of a solute in a supercritical solvent to the density, temperature, and/or pressure.¹³ The form of empirical Chrastil model is shown in eq 2, based on the hypothesis that the solute molecule combination with the supercritical solvent molecules produces solvate complexes in terms of the following equilibrium 1:



where A stands for solute and B for solvent.¹²

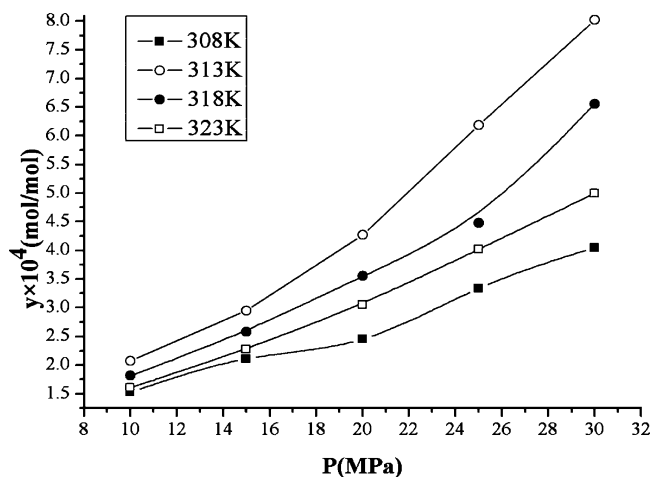
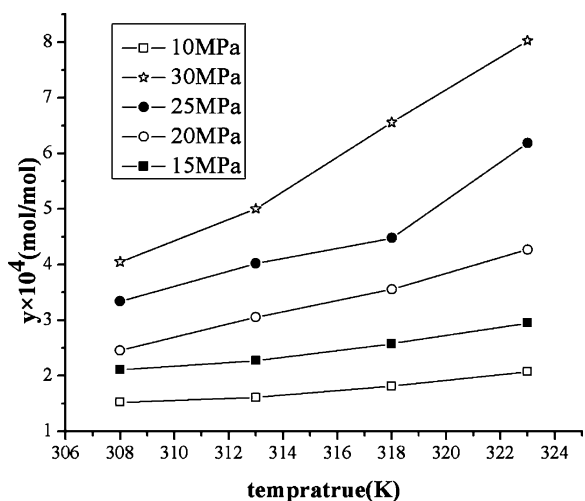
Equations 4 and 5 are modifications of Chrastil. In all the modified and unmodified Chrastil models, *S* is the solubility of the solute in the SC-CO₂ (g·L⁻¹); ρ is the density of pure carbon dioxide (kg·m⁻³); *T* is the temperature in K; and parameter *k* is the association number of carbon dioxide. Parameter *a* depends on the total reaction enthalpy; β is a parameter depending on the molecular weights and melting points of the solute and solvent. Analogously to the interpretation given by Yusuke Shimoyama, the process of solid solute dissolution in the supercritical solvent can include

Table 1. Comparison of the Obtained Solubility (*y*) of Naphthalene in SC-CO₂ at 308.0 K with Those of Ref 10

P/MPa	this work	ref	P/MPa	this work	ref	P/MPa	this work	ref
8.0	0.0041	0.0044	20.0	0.0158	0.0161	30.0	0.0172	0.0175
15.0	0.0145	0.0147	25.0	0.0168	0.0169			

Table 2. Experimental Solubility of DL-2-Phenoxypropionic Acid in SC-CO₂

T/K	P/MPa	$\rho/\text{kg}\cdot\text{m}^{-3}$	$10^4 y$	T/K	P/MPa	$\rho/\text{kg}\cdot\text{m}^{-3}$	$10^4 y$
308.0	10.0	668.40	1.5256	318.0	10.0	484.26	1.8158
308.0	15.0	797.26	2.1082	318.0	15.0	711.97	2.5783
308.0	20.0	866.48	2.4535	318.0	20.0	802.33	3.5573
308.0	25.0	915.52	3.3383	318.0	25.0	862.07	4.4783
308.0	30.0	954.03	4.0477	318.0	30.0	907.03	6.5553
313.0	10.0	586.04	1.6083	323.0	10.0	391.81	2.0749
313.0	15.0	755.88	2.2748	323.0	15.0	666.06	2.9490
313.0	20.0	834.91	3.0541	323.0	20.0	769.10	4.2703
313.0	25.0	889.07	4.0179	323.0	25.0	834.44	6.1835
313.0	30.0	930.63	5.0002	323.0	30.0	883.18	8.0237

Figure 3. Effect of pressure on the experimental solubility of DL-2-phenoxypropionic acid in SC-CO₂.Figure 4. Effect of temperature on the experimental solubility of DL-2-phenoxypropionic acid in SC-CO₂.

two steps: the solid solute vaporizes into a fluid state and the fluid solute associates with the supercritical solvent molecules.¹⁴ While as the state of conglomeration is diverse, the relationship between heat capacity and temperature is variational. The Del Valle and Aguilera modification of eq 4 to the Chrastil model introduced a parameter to correct the α , taking vaporator heat changed to temperature into account. Adachi and Lu considered the k as a dynamic parameter and introduced two density dependent parameters to modify it as eq 5.¹⁵

In Mendez-Santiao and Teja equation $T \ln(y_2 P / P^{\text{std}}) = \beta + k\rho + \alpha T$ (eq 6), P is the operation pressure, and P^{std} is the standard pressure. The significations of parameter k , α , and β are different from those of the Chrastil equation.

The correlation models aforementioned and correlated results of experimental data are shown in Table 3. It can be observed that the Chrastil correlation and its modifications produce more acceptable precisions than those of the Mendez-Santiago and Teja equation. The values of α in modified and unmodified Chrastil equations indicate that the dissolution of DL-2-phenoxypropionic acid in SC-CO₂ is an endothermic process.¹³ Compared to the Chrastil model, Del Valle and Aguilera modification does not improve the correlation accuracy markedly. This may interpret that the solubility is not strongly dependent on the total reaction enthalpy. While the results from eq 5 demonstrate that the correlation effect is quite satisfactory, the change of association number k depending on ρ evidently influences the solubility. However, those modifications still neglect the fact that the association reaction equilibrium can change with the pressure and temperature.¹⁶

Effect of Pressure on Solubility of DL-2-Phenoxypropionic Acid. It can be easily seen from Figure 3 that the solubility of DL-2-phenoxypropionic acid increases with the rise in pressure at a constant temperature. The rise in pressure increases the solvent density and results in an increase of solubility due to the stronger solute solvent interactions.¹⁷ And the association number k depending on ρ may also increase according to eq 5. In addition, another possible reason for the increasing solubility is the promoted association reaction at the higher pressure. As in the equilibrium (2), A (DL-2-phenoxypropionic acid) is solid, B and AB_k are fluids, theoretically k is greater than 1, the reaction will shift toward products with the increase of pressure according to the theory of chemical equilibrium.

Effect of Temperature on Solubility of DL-2-Phenoxypropionic Acid. The effect of increasing temperature on the solute solubility depends on the result of the competing effect of increasing solute vapor pressure and decreasing solvent density. On the one hand, as the temperature increases, the solvent density decreases, and therefore the solute solubility decreases. On the other hand, with the increase of temperature, the volatility of solute improves and therefore raises the solubility.¹⁷ It is obviously shown in the Figure 4 that the solubility increases with the increase of temperature over this experimental range as in the results reported by Junsu Jin et al.,¹⁸ which means in the currently experimental pressure range from (10 to 30) MPa, the vapor pressure effect is always dominant in the system. What is more, the increase in temperature will make the association reaction proceed in a

Table 3. Values of Parameters Used for Solubility Model and Average Absolute Relative Deviations

model	eq	β	k	α	AARD
Chrastil model	$\ln S = \beta + k \ln \rho + (\alpha/T)$ (3)	-0.6372	2.8132	-5707.3	0.1555
del Valle and Aguilera/Chrastil	$\ln S = \beta + k \ln \rho + (\alpha_1/T) + (\alpha_2/T^2)$ (4)	100.8154	2.8167	$\alpha_1 = -69\,715$ $\alpha_2 = 10\,090\,000$	0.1523
Adachi and Lu/Chrastil	$\ln S = \beta + k \ln \rho + (\alpha/T)$ where $k = k_1 + k_2\rho + k_3\rho^2$ (5)	-10.7568	$k_1 = 5.4218$ $k_2 = -0.002364$ $k_3 = -0.0000014321$	-5999.1	0.0532
Mendez-Santiao and Teja	$T \ln(y_2P/P^{\text{std}}) = \beta + k\rho + \alpha T$ (6)	-9566.3	1.7653	23.1616	0.1865

forward direction as the association reaction is an endothermic process.

As the Adachi and Lu modified Chrastil model provides an appreciable accuracy with AARD of 0.0532, the change of solubility with temperature and pressure can be obviously described by the Figure 5, and, most important, the figure

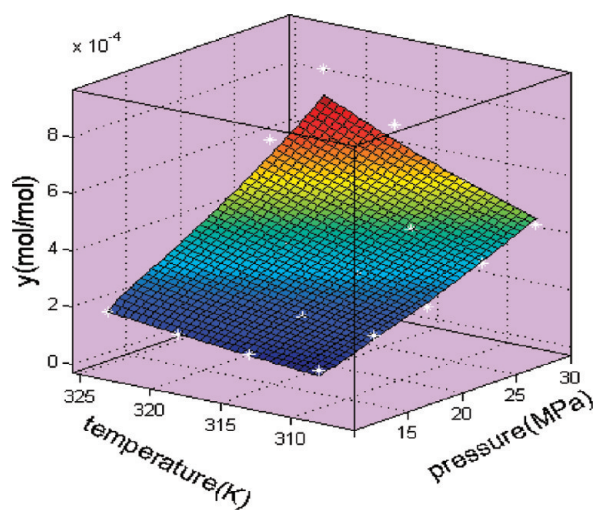


Figure 5. Effect of temperature and pressure on the solubility of DL-2-phenoxypropionic acid in SC-CO₂ calculated with the Adachi and Lu modified Chrastil model (white points are experimental solubility data).

indicates that the calculated results are in good agreement with the experimental data, which confirms that the mole fraction solubility of DL-2-phenoxypropionic acid under SC-CO₂ is up to 10⁻⁴, and so, the RESS process on DL-2-phenoxypropionic acid is completely valuable and available.

RESS. The results of the nanosize structures in comparison with the original DL-2-phenoxypropionic acid crystalline form are seen in Figure 6. The first figure indicates that the untreated particles have no formula shape and no uniformity size with irregularity surface and equivalent diameters between (10 and 50) μm , while other pictures show that microstructures produced by RESS are filaments entwining into mesh pattern with the diameter of (1 to 15) nm, and even flakes and particles in some cases. The exact sizes and shapes vary depending on the different temperatures, pressures, nozzle sizes, and spray distances. Similar experiments and phenomena were reported by Hezave et al.^{5-9,19,20} However, the variety in size is not dramatic in this study, but the change in shape there is rather great.

Effect of Nozzle Diameter. In this study, nozzle diameter ranged from (0.1 to 0.2 and 0.4) mm; the other parameters including extraction pressure (30 MPa), extraction temperature (323 K), nozzle temperature (363 K), and spray distance (20

mm) were held constant. The filament diameters of DL-2-phenoxypropionic acid increase as nozzle diameters increase from (0.1 to 0.4) mm as shown obviously in SEM images of Figure 6d,b,c. When the nozzle diameter was 0.1 mm, the diameters of filaments were between (1 and 5) nm. As the nozzle rose to 0.4 mm, the filaments can increase to 15 nm. The increasing sizes can be explained as follows: it will shorten the time for the saturated fluid to go through the nozzle, prolong the expansion time, and lower the nucleation rate. So, the precipitated particles will be smaller in size.⁶ Similar results have been observed for the case of chitin, cephalixin, and ketoprwfen.⁶⁻⁸ However, the result is contrary to the conclusion of Michael Türk.³

Effect of Spray Distance. Spray distance to the collection plane is another key to control the particle size. In this research, five experiments with the spray distances changed from (10 to 15, 20, 25, and 30) mm at the extraction parameters of 323 K and 30 MPa, nozzle temperature of 363 K, and nozzle diameter of 0.1 mm were conducted. The SEM images of processed DL-2-phenoxypropionic acid structures of (10, 20, and 30) mm spray distances, given in Figure 6e,d,f separately, indicate that the diameters of filaments over all the above-mentioned spray distances were within (1 to 10) nm. The increase of spray distances results in an increase in the average diameters, although the variety is not as apparent as influenced by nozzle diameter, and the increasing spray distance is in favor of the filament dispersing to individual microstructure in entwined form, even in flake form.¹⁹ A larger distance means an increasing time for fluid residence in the expansion space, which leads to longer time for particle growth, and therefore bigger size structures.^{6,20} This is one aspect of this matter; in another aspect, when the spray distance is long enough, the agglomeration can be avoided due to the increasing angles between particles⁹ and enough time for SC-CO₂ to change from a supercritical solvent to usual CO₂ gas and disperse. So, the increase of the DL-2-phenoxypropionic acid microstructure size and the trend of individual structures with the increasing spray distances can be attributed to these two phenomenons in this article.

Effect of Extraction Pressure. SEM photographs of the influence of extraction pressure on DL-2-phenoxypropionic acid given in Figure 6g,h,i are of (10, 20, and 30) MPa at the extraction temperature of 308 K, nozzle temperature of 363 K, nozzle diameter of 0.1 mm, and collection distance of 20 mm. The filaments are sprinkled with irregular particles at an extraction pressure of 10 MPa. There are some fine spherical particles distributing along filaments when the extraction pressure is 20 MPa. The most surprising thing about it is that the microstructures are flake interconnected with filaments at 30 MPa. The results depicted above clarify that extraction pressure plays an important role in the product dominating morphology formation. There is also indication on the change

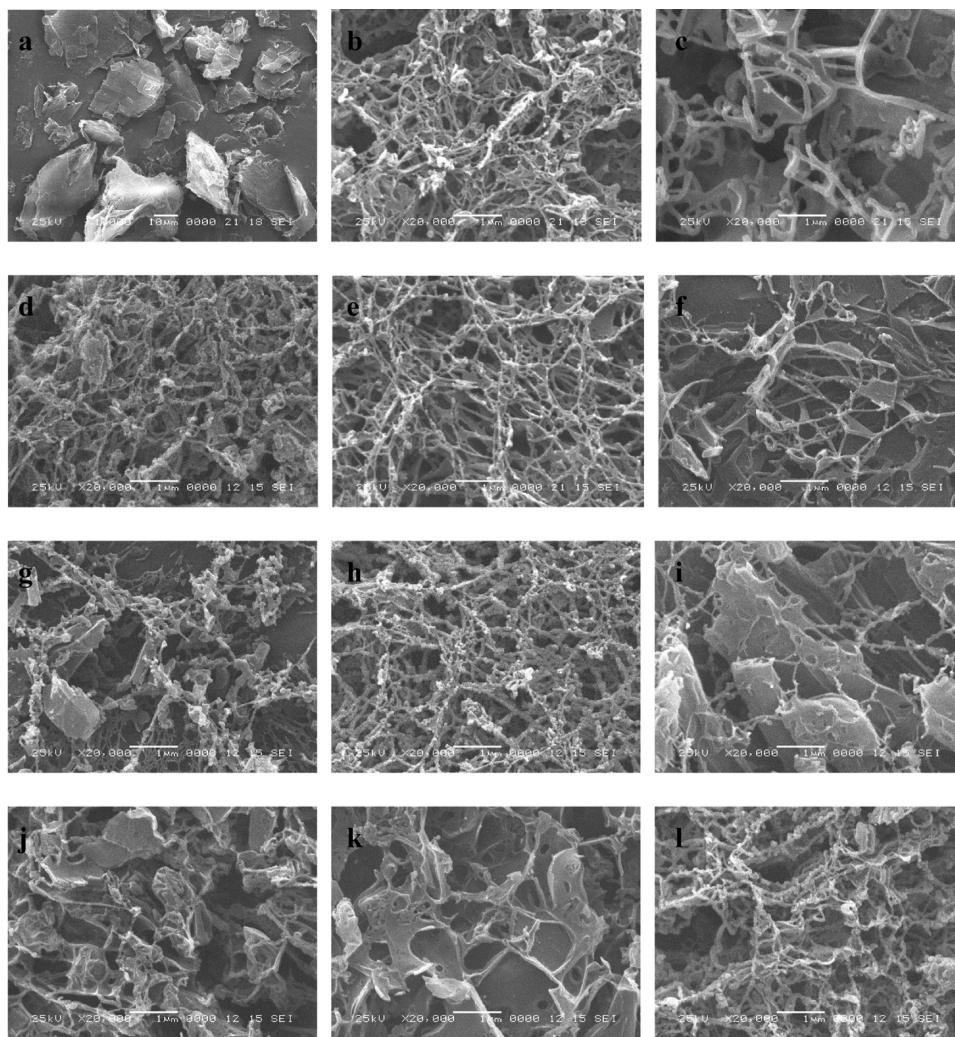


Figure 6. SEM images of DL-2-phenoxypropionic acid microstructures unprocessed and processed by RESS.

of filament sizes: the filament diameters decrease from about (8 to 1) nm as the extraction pressures increase from (10 to 30) MPa. Increasing the extraction pressure leads to the increase of DL-2-phenoxypropionic acid solubility in the SC-CO₂ as illustrated in Figure 3 and leads therefore to a rise in the degree of supersaturation at the expansion moment. Michael Türk pointed out that rates of particle nucleation and growth were influenced by supersaturation to different degrees. The nucleation rate is linear in supersaturation, which depends on the supersaturation more strongly than that of the growth rate.³ Nevertheless, the effect of pressure on solubility dominates the process over the operation conditions in this study, and hence, the smaller filaments were found at the higher extraction pressure, which is familiar to results observed by Nuray Yildiz et al.²⁰ However, it is inconsistent with the classical nucleation theory, according to which the lower solubility would cause the reducing of nucleation rates and decrease of particle size due to the delay of precipitation and/or a smaller number of particle encounters in the expansion process.¹ At the same time, higher extraction pressure always combines with more intense expansion, which shortens the residence time and meanwhile aggravates particle collision. This is why the flakes were obtained at 30 MPa, while at 10 MPa, the dominant structures were filaments and particles.

Effect of Extraction Temperature. The influence of extraction temperature on morphology and size of DL-2-phenoxypropionic acid microstructures was performed at varying extraction temperatures ((308, 313, 318, 323, and 328) K), while the other parameters included nozzle temperature of 363 K, nozzle diameter of 0.1 mm, spray distance of 20 mm, and extraction pressure of 30 MPa. The pictures of (308, 318, and 323) K extraction temperature are exhibited in Figure 6(i,j,d), respectively. With the increase of extraction temperature, both the number and size of the flake decreases, and the filaments turn to be close together and the amount increases. When the extraction temperature is up to 323 K from the initial 308 K, the formations completely changed from flakes to filaments. The possible reason for this, from results published in the literature^{3,20} and the term in which extraction pressure influences particle formation illustrated above, is that one could expect that filament diameter decreases with the increase of temperature; and when the diameter decreased to a certain value, flakes turned to filaments gradually. Besides, what is worthy to be clarified is that higher solubility brings higher nucleation rate, which concurrently induces particle collision.

Effect of Nozzle Temperature. The investigation of the nozzle temperature effect on DL-2-phenoxypropionic acid precipitation was made for three separate temperatures ((343, 363, and 383) K). As illustrated in Figure 6(k,d,l), extraction

conditions of 30 MPa and 323 K, nozzle diameter of 0.1 mm, spray distance 20 mm, and nozzle temperatures of (343, 363, and 383) K, with the increase of nozzle temperature, DL-2-phenoxypropionic acid morphology changed from flakes mixed with filaments to absolute filaments; meanwhile, filament diameter first decreases from (8 to 5 to 1) nm approximately, then slightly increases to (3 and 5) nm, the minimum diameter is at the nozzle temperature of about 363 K. The decreasing diameters may be due to the rise in solubility and consequent decrease in supersaturation, which delays the precipitation and particle formation of solute in the nozzle as the nozzle temperature increases.⁹ The morphology change from flakes to filaments can be explained by the improved dispersion due to the increasing temperature.

The above-mentioned research results show that the trend of particle size change can be explained by the variety of solubility and dispersion to some degree. However, just as the opinion of Reverchon, the observed particle morphologies had to be explained by the interaction among fluid dynamics, phase equilibria at high pressure, and mass transfer during the RESS process.²¹ It is insufficient to accurately predict particle characters only by solubility knowledge for it is just one aspect of this problem.

CONCLUSIONS

The solubility of DL-2-phenoxypropionic acid in supercritical CO₂ increases with the increase of pressures at a settled temperature and the increase of temperature at a constant pressure. Besides, the correlated results show that the Chrastil model and its modifications have a better correlation effect than that of the Mendez-Santiago and Teja equation. From the RESS part of the experiments, we can conclude that fine and shape regular DL-2-phenoxypropionic acid microstructures can be carried out with RESS. The effect of process conditions, including extraction temperature and pressure, nozzle temperature, nozzle diameter, and spray distance, on the microstructures of DL-2-phenoxypropionic acid particles was investigated, and it is found that the aforementioned parameters influence the particle size and morphology to different extents. The solubility data are critical information for RESS process since the temperature and pressure have an affect on RESS mainly through influencing DL-2-phenoxypropionic acid solubility so as to affect the degree of supersaturation, and there is a general trend that it is beneficial to obtain smaller particle when the operator conditions cause higher supersaturation. The nozzle size and spray distance influence microstructure size more strongly than the temperature and pressure do, while the latter two play a more important role in the shape of microstructures in this research.

AUTHOR INFORMATION

Corresponding Author

*Tel/Fax: 86-0730-8640122. E-mail: YJM91@163.com.

Funding

This work was supported by the National Science Foundation of China (No. 21076068) and by the Hunan Provincial Natural Science Foundation of China (No. 07JJ3016).

REFERENCES

(1) Breining, E.; Imranulhaq, M.; Türk, M.; Beuermann, S. Effect of polymer properties on poly (vinylidene fluoride) particles produced by rapid expansion of CO₂ + polymer mixtures. *J. Supercrit. Fluids* **2009**, *48*, 48–55.

(2) Kongsombut, B.; Tsutsumi, A.; Suankaew, N.; Charinpanitkul, T. Encapsulation of SiO₂ and TiO₂ fine powders with poly(dl-lactic-co-glycolic acid) by rapid expansion of supercritical CO₂ incorporated with ethanol cosolvent. *Ind. Eng. Chem. Res.* **2009**, *48*, 11230–11235.

(3) Türk, M. Manufacture of submicron drug particles with enhanced dissolution behaviour by rapid expansion processes. *J. Supercrit. Fluids* **2009**, *47* (3), 537–545.

(4) Calderone, M.; Tallon, S. Particle formation by rapid expansion from solution using near-critical dimethyl-ether. *J. Supercrit. Fluids* **2008**, *45*, 245–252.

(5) Hezave, A. Z.; Esmailzadeh, F. Crystallization of microparticles of sulindac using rapid expansion of supercritical solution. *J. Cryst. Growth* **2010**, *312* (22), 3373–3383.

(6) Hezave, A. Z.; Esmailzadeh, F. Investigation of the rapid expansion of supercritical solution parameters effects on size and morphology of cephalexin particles. *J. Aerosol Sci.* **2010**, *41* (12), 1090–1102.

(7) Ricardo, S. H.; Ruiz-Trevino, F. A.; Estrada, C. H. O. Chitin microstructure formation by rapid expansion techniques with supercritical carbon dioxide. *Ind. Eng. Chem. Res.* **2009**, *48* (2), 769–778.

(8) Hezave, A. Z.; Aftab, S.; Esmailzadeh, F. Micronization of ketoprofen by the rapid expansion of supercritical solution process. *J. Aerosol Sci.* **2010**, *41*, 821–833.

(9) Atila, C.; Yildiz, N.; Calimli, A. Particle size design of digitoxin in supercritical fluids. *J. Supercrit. Fluids* **2010**, *51*, 404–411.

(10) Sauceau, M.; Fages, J.; Letourneau, J. J.; et al. A novel apparatus for accurate measurements of solid solubilities in supercritical phases. *Ind. Eng. Chem. Res.* **2000**, *39* (12), 4609–4614.

(11) Peng, D. Y.; Robinson, D. A new two-constant equation of state. *Ind. Eng. Chem. Fundam.* **1976**, *15*, 59–64.

(12) Fan, J.; Hou, Y.; Wu, W.; Zhang, J.; Ren, S.; Chen, X. Levulinic acid solubility in supercritical carbon dioxide with and without ethanol as cosolvent at different temperatures. *J. Chem. Eng. Data* **2010**, *55*, 2316–2322.

(13) Hassan, S. G.; Mohammad, K. Solubility of trioctylamine in supercritical carbon dioxide. *J. Supercrit. Fluids* **2008**, *44*, 148–154.

(14) Shimoyama, Y.; Higashi, H.; Tsuzaki, S.; Okazaki, F.; Kitani, Y.; Iwai, Y.; Arai, Y. Effect of cation species on solubilities of metal chlorides in water vapor at high temperatures and pressures. *J. Supercrit. Fluids* **2009**, *50*, 1–5.

(15) Lucas, A.; Gracia, I.; Rincon, J.; Garcia, M. T. Solubility determination and model prediction of olive husk oil in supercritical carbon dioxide and cosolvents. *Ind. Eng. Chem. Res.* **2007**, *46*, 061–066.

(16) Jiang, C.; Pan, Q.; Pan, Z. Solubility of styrene in supercritical carbon dioxide. *J. Chem. Ind. Eng.* **2002**, *53* (7), 723–728.

(17) Song, Q.; Zhu, J.; Wan, J.; Cao, X. Measurement and modeling of epigallocatechin gallate solubility in supercritical carbon dioxide fluid with ethanol cosolvent. *J. Chem. Eng. Data* **2010**, *55*, 3946–3951.

(18) Jin, J.; Pei, X.; Li, J.; Zhang, Z. Solubility of *p*-amino-benzenesulfonamide in supercritical carbon dioxide with acetone cosolvent. *J. Chem. Eng. Data* **2009**, *54*, 157–159.

(19) Jun, H. K.; Hullathy, S. G.; Seung, S. H.; Yeong, S. G.; Kwon, T. L. Preparation of polyacrylonitrile nanofibers as a precursor of carbon nanofibers by supercritical fluid process. *J. Supercrit. Fluids* **2008**, *47*, 103–107.

(20) Yildiz, N.; Tuna, S.; Doker, O.; Calimli, A. Micronization of salicylic acid and taxol (paclitaxel) by rapid expansion of supercritical fluids (RESS). *J. Supercrit. Fluids* **2007**, *41*, 440–451.

(21) Reverchon, E. Interactions of phase equilibria, jet fluid dynamics and mass transfer during supercritical antisolvent micronization. *Chem. Eng. J.* **2010**, *56* (2), 446–458.